

Tectonic Activity on Pluto After the Charon-Forming Impact

Amy C. Barr^a, Geoffrey C. Collins^b

^a*Brown University, Dept. of Geological Sciences, Providence, RI 02912, USA*

^b*Department of Physics and Astronomy, Wheaton College, Norton, MA 02776, USA*

Abstract

The Pluto-Charon system, likely formed from an impact, has reached the endpoint of its tidal evolution. During its evolution into the dual-synchronous state, the equilibrium tidal figures of Pluto and Charon would have also evolved as angular momentum was transferred from Pluto's spin to Charon's orbit. The rate of tidal evolution is controlled by Pluto's interior physical and thermal state. We examine three interior models for Pluto: an undifferentiated rock/ice mixture, differentiated with ice above rock, and differentiated with an ocean. For the undifferentiated case without an ocean, the Pluto-Charon binary does not evolve to its current state unless its internal temperature $T_i > 200$ K, which would likely lead to strong tidal heating, melting, and differentiation. Without an ocean, Pluto's interior temperature must be higher than 240 K for Charon to evolve on a time scale less than the age of the solar system. Further tidal heating would likely create an ocean. If *New Horizons* finds evidence of ancient tidally-driven tectonic activity on either body, the most likely explanation is that Pluto had an internal ocean during Charon's orbital evolution.

Keywords:

1. Introduction

As the *New Horizons* spacecraft travels toward the Pluto/Charon system, our knowledge about the system’s physical properties (Olkin et al., 2003; Gulbis et al., 2006; Tholen et al., 2008), mode of formation (Canup, 2005, 2011), and surface composition (e.g., Olkin et al. 2003; Brown and Calvin 2000; Buie and Grundy 2000; Cook et al. 2007) continues to grow. The general properties of the Pluto and Charon system, including its dynamical state and the Pluto-to-Charon mass ratio, suggest that Charon may have formed due to a collision between two like-sized precursor objects (Canup, 2005, 2011). Careful examination of the system in preparation for the *New Horizons* mission has led to the discovery of four additional small moons, Nix, Hydra (Weaver et al., 2006), Styx, and Kerberos (Showalter et al., 2011, 2012). The moons are in mean motion resonances with Charon (Weaver et al., 2006; Stern et al., 2006; Buie et al., 2006; Showalter et al., 2013), which could imply that they formed by accretion of debris after the Charon-forming impact or were captured (Ward and Canup, 2006; Kenyon and Bromley, 2014).

The Pluto/Charon system is unique among major bodies in the solar system because it has reached the endpoint of its dynamical evolution: the so-called “dual synchronous” state in which Charon’s orbital period, spin period, and Pluto’s rotation period are equal; Charon currently orbits Pluto at $a_c \sim 16.4R_P$, where $R_P = 1147$ km is Pluto’s radius (Tholen et al., 2008). As the orbit evolved to its present state and Pluto’s spin rate changed to match Charon’s orbital period, changes in the equilibrium tidal and rotational figures of the two bodies may have left their mark as systems of tectonic features on the surfaces of each body. Orbit and spin evolution of the Pluto/Charon

system is driven by the raising and lowering of tidal bulges on each body. The tidal bulges exert torques which change the semi-major axes of the orbits and the spin rates. The mechanical energy associated with the periodic raising and lowering of the bulges is dissipated as heat in the bodies' interiors. Changes in bulge height and energy dissipation are thought to drive endogenic resurfacing and tectonic activity on many of the icy satellites of the outer solar system (see, e.g., Schubert et al. 1986; Peale 1986; Greeley et al. 2004 for discussion). The magnitude of stresses arising from tidal evolution depends on the interior structures of the bodies and the frequency of tidal flexing; the frequencies in turn depend on the Pluto/Charon distance and the spin periods. The main source of stress accumulation in the Pluto/Charon system would be figure changes associated with transfer of momentum from Pluto's spin to Charon's orbit. If the stresses exerted on the surfaces of the bodies exceed the nominal yield stress of ice, we consider that tectonic activity may have occurred. The presence or absence of tectonic features, along with their distribution and orientations, may provide clues about the early evolution of the system (Collins and Pappalardo, 2000). Thus, images of the surfaces of Pluto and Charon from *New Horizons* could yield clues about the post-impact interior state of Pluto and the initial orbital distance of Charon.

In successful hydrodynamical simulations of the Charon-forming impact, Charon is launched into an eccentric orbit around a rapidly spinning Pluto (cf. Dobrovolskis et al. 1997); its initial orbital semi-major axis after the impact, a_o , ranges from $\sim 3.7R_P$ to $21R_P$ (Canup, 2008). Over a time scale $\tau_{synch} \sim 35(Q_c/100)$ years (Dobrovolskis et al., 1997), where $Q_c \sim 100$ is a nominal estimate of Charon's tidal quality factor, Charon evolves to

a synchronous state in which its spin period and orbital period are equal (similar to the Earth-Moon system). The final migration from the synchronous state to the dual-synchronous state takes much longer, $\Delta t_{evol} \approx 200(Q_p/100)(10^{-3}/k_{2,p})\text{Myr}$, where Q_p is Pluto's tidal quality factor, and $k_{2,p}$ is the degree-2 Love number that describes how Pluto's gravitational potential changes in response to the tides raised on Pluto by Charon.

In this work, we calculate the migration timescale and stresses generated in Pluto's lithosphere due to the orbital evolution of the system from its initial post-impact state to its present dual-synchronous state. We determine the Love numbers of Pluto as a function of its interior structure, temperature, and the time scale of deformation. The Love numbers are used to estimate its Q immediately post-impact, and to determine the magnitude of tidal deformation in a rapidly spinning Pluto. The Love numbers are also used to constrain the magnitude of deformation and stresses built up in Pluto's lithosphere. The Q values based on realistic interior structures for Pluto are used to constrain the orbital evolution time scale of the system and the rate of deformation associated with decreasing Pluto's tidal bulge as Charon recedes. Assuming nominal parameters describing the brittle and ductile behavior of water ice (e.g., Table 2), we determine the conditions under which the induced stresses and deformation rates can fracture Pluto's surface, and determine how that likelihood varies as a function of Pluto's thermal state post-impact.

2. Background

The discovery of new satellites in the Pluto system has provided new constraints on the masses of Pluto and Charon. Table 5 summarizes the present-day knowledge of the physical properties of the system based on a four-body orbital solution from Tholen et al. (2008), which also incorporates prior information about Pluto’s radius from stellar occultation data (e.g., Olkin et al. 2003; Gulbis et al. 2006). The current estimate for the mean density of Pluto is $\bar{\rho}_p = 2060 \text{ kg m}^{-3}$ (Tholen et al., 2008; Canup, 2011). The spin/orbital period of Charon at present is 6.38720 days (Tholen et al., 2008). In the dual-synchronous state, the spin frequency of Pluto (ω_p), Charon (ω_c), and orbital frequency of Charon (n_f) are the same, so that $\omega_p = \omega_c = n_f = 1.139 \times 10^{-5} \text{ s}^{-1}$. Charon orbits Pluto at a distance of $a_f = 16.4R_p$.

It is commonly held that Charon formed in an impact between two like-sized precursor ice/rock bodies (Canup, 2005, 2011). Simulations of the impact which produce the proper mass and mean density for Charon show that the object striking proto-Pluto must be undifferentiated at the time of impact to create Charon’s mixed ice/rock composition (Canup, 2005). No such constraints exist for the differentiation state of Pluto; a collision between undifferentiated objects is consistent with the present-day masses and densities of each object. The energy rise associated with the impact is modest, with the interior of Pluto being heated by $\Delta T \sim O(10 - 100) \text{ K}$, and Charon’s interior being heated by $\Delta T \sim 30 \text{ K}$ (Canup, 2005). It appears likely that the interiors of either object could be heated to within a few tens of degrees Kelvin of their melting points by long-lived radiogenic heating before the impact, particularly if their interiors contain ammonia, which

would decrease the melting points of their icy components (Husmann et al., 2006; McKinnon et al., 2008).

The evolution of the binary system to the dual-synchronous state is controlled by the tides raised on Pluto due to Charon’s orbit (Dobrovolskis et al., 1997). If Charon’s $a_o < 16.4R_p$, angular momentum is transferred from Pluto’s spin to Charon’s orbit, causing Charon to evolve outward as Pluto de-spins. If Charon’s $a_o > 16.4R_p$, angular momentum is transferred from Charon’s orbit to Pluto’s spin, and Charon moves closer to Pluto until it achieves the dual-synchronous state. Tides within Pluto are raised and lowered with a frequency $\omega_{tidal} = \omega_p - n$, where ω_p and n are the spin frequency of Pluto and Charon’s mean motion, respectively, both of which change during orbital evolution.

Immediately following the Charon-forming impact, we assume that Charon is launched into a highly eccentric, co-planar orbit around a rapidly spinning Pluto (cf. Dobrovolskis et al. 1997); this eccentricity is damped rapidly. Assuming a constant tidal quality factor for Pluto, the change in Charon’s mean motion due to the torque between Pluto and Charon is related to their physical properties as (Dobrovolskis et al., 1997),

$$\frac{dn}{dt} = -\frac{9}{2} \frac{k_{2,p}}{Q} \frac{m_c}{m_p} \frac{R_p^5 n^{16/3}}{[G(m_p + m_c)]^{5/3}}, \quad (1)$$

where m_p is Pluto’s mass, m_c is Charon’s mass, $k_{2,p}$ is Pluto’s degree-2 Love number describing the change in Pluto’s gravitational potential due to its distortion, and Q is Pluto’s tidal quality factor. Assuming a constant Q as a function of time, equation (1) can be integrated to give the time scale of

orbital evolution for the system (cf. Dobrovolskis et al. 1997),

$$\tau_{evol} = \frac{2}{39} \frac{Q}{k_{2,p}} \frac{m_p}{m_c} \frac{[G(m_p + m_c)]^{5/3}}{R_p^5} (n_f^{-13/3} - n_o^{-13/3}), \quad (2)$$

where $n_o = (Gm_p/a_o^3)^{1/2}$ is the mean motion of Charon immediately post-impact. For the minimum $a_o/R_p \sim 3.7$ (which gives $n_o \sim 10^{-4} \text{ s}^{-1}$), nominal estimates for Q and $k_{2,p}$, and $n_f = 1.13 \times 10^{-5} \text{ s}^{-1}$, equation (2) gives $\tau_{evol} \sim 200 \text{ Myr}$. As discussed in section 3.3, the value of Q is dependent on the frequency of tidal deformation and the interior state of Pluto. Therefore, an overall τ_{evol} based on a constant Q should be regarded only as an initial estimate that does not use the full information available.

A crude estimate of the tidal distortion of Pluto during its early period of rapid rotation can shed light on the stresses exerted in its lithosphere during this early phase of orbital evolution. The magnitude of the strain, ε , on Pluto's lithosphere due to the tidal deformation is also related to $k_{2,p}$ and the system properties (Love, 1944; Dobrovolskis et al., 1997),

$$\varepsilon = \frac{\delta r}{R_p} = \frac{5}{3} k_{2,p} \frac{m_c}{m_p} \left(\frac{R_p}{a_o} \right)^3 \sim 3\% \left(\frac{k_{2,p}}{0.001} \right), \quad (3)$$

for $a_o \sim 3.7R_p$ and a nominal $k_{2,p} \sim O(10^{-3})$ (Dobrovolskis et al., 1997). This implies stresses of order $\sigma \sim 2\mu\varepsilon \sim 100 \text{ MPa}$, where $\mu = 3.6 \times 10^9 \text{ Pa}$ is the shear modulus for water ice. These stresses are significantly higher than the $\sim 0.1 \text{ MPa}$ yield stress of polycrystalline water ice inferred from terrestrial ice sheets (Kehle, 1964), and higher than the yield stress of the lithosphere of Europa inferred from the models of the formation of its tectonic features (Hoppa et al., 1999; Stempel et al., 2005; Hurford et al., 2007). It is also higher than the $\sim 2 \text{ MPa}$ tensile strength of polycrystalline water ice at temperatures found in the outer solar system (Litwin et al., 2012).

This suggests that stresses from figure change may be sufficient to fracture Pluto’s surface and create tectonic features (Collins and Pappalardo, 2000) that could be observable by *New Horizons*.

3. Methods

Here, we estimate the time scale of orbital evolution from the synchronous to dual-synchronous state as a function of the interior viscosity of Pluto for three different interior states: a differentiated Pluto with an ocean, a differentiated Pluto without an ocean, and an undifferentiated Pluto (see Figure 2). We derive a time estimate by integrating the constant- Q approximation in equation (2) for small steps in the Pluto-Charon distance, varying Q as a function of distance. We calculate Love numbers for Pluto assuming a radially symmetric structure and vary the thermal state by using different values for the viscosity of ice in the interior. Finally, we calculate the magnitude of surface stresses available to drive tectonic activity by assuming deformation of a thin elastic shell (Melosh, 1977) due to changes in the equilibrium figures of Pluto and Charon as orbital evolution proceeds.

3.1. Interior Models

Figure 2 illustrates the three simple models we consider for the interior structure of Pluto immediately after the Charon-forming impact: a homogeneous (uniform-density) interior, a fully differentiated and solid interior, and a fully differentiated interior with an ocean. Table 5 summarizes the physical properties of Pluto.

We assume that Pluto is composed primarily of water ice with a density $\rho_i = 1000 \text{ kg m}^{-3}$, slightly higher than the density of cold, pure water ice

(Mueller and McKinnon, 1988) to account for the possible inclusion of hydrocarbons and higher-density N-bearing compounds (McKinnon et al., 1997, 2008). We assume that its rocky component has a density $\rho_r = 3000 \text{ kg m}^{-3}$, mid-way between the grain density of CI chondrite ($\rho_r = 2800 \text{ kg m}^{-3}$) and Prinn/Fegley rock ($\rho_r = 3300 \text{ kg m}^{-3}$), which are two models for the composition of the rocky components of large icy moons (Mueller and McKinnon, 1988). With our choices of rock and ice densities, Pluto has a volume fraction of rock $\phi = (\bar{\rho} - \rho_i)/(\rho_r - \rho_i) = 0.53$, consistent with more detailed structural models of McKinnon et al., (2008).

Not much is known about the interior state of Pluto before the Charon-forming impact. Much of the prior work on Pluto’s interior assumes that it differentiated during its formation and early history (McKinnon et al., 1997, 2008; Robuchon and Nimmo, 2011). However, simulations of the Charon-forming impact show that the proper mass, composition, and angular momentum for the system is most readily obtained when Pluto and the Charon-forming impactor are only partially differentiated (Canup, 2005, 2011).

Here, we consider both cases as a possibility, but we favor differentiated Plutos. The gravitational binding energy associated with assembling Pluto, $3/5(GM_P/R_P) \sim 4.5 \times 10^5 \text{ J/kg}$ (where M_P is Pluto’s mass) is larger than the latent heat of water ice, $L \sim 3 \times 10^5 \text{ J/kg}$, suggesting that Pluto’s ice could melt during its accretion if 100% of its accretional energy were retained as heat. This may not be the case, especially if Pluto formed slowly, and from low-velocity impacts (see e.g., Ahrens and O’Keefe 1977). If Pluto formed very early in solar system history, before the dissipation of the solar nebula ($\sim 10 \text{ Myr}$), comparable to the lifetime of disks

around other stars (Haisch et al., 2001; Thi et al., 2001), it may have been heated by the short-lived radioisotopes (SLRI) ^{26}Al and ^{60}Fe , which have half-lives less than ~ 1 Myr and are present in greater abundances than U, Th, and K (Tachibana and Huss, 2003; Lodders, 2003; Mostefaoui et al., 2004; Bizzarro et al., 2005; Thrane et al., 2006; Wadhwa et al., 2007). SLRI are particularly efficient at driving differentiation because they release heat on a time scale much shorter than the time scale for diffusive or convective heat transport in Pluto’s interior. Removing a heat pulse from short-lived radioisotope decay across the outer $\delta \sim 500$ km of Pluto’s interior would require $\tau_{diff} \sim \delta^2/\kappa \sim 7$ Gyr, where $\kappa \sim 10^{-6}$ m²/s is the thermal diffusivity of water ice. Solid-state convection could provide more efficient heat transport, but the time scale for the first convective overturn in Pluto’s deep interior (Zarank and Parmentier, 2004),

$$t_o = \frac{500}{\kappa} \left(\frac{\rho \alpha_T \Delta T_i g}{\eta_o \kappa} \right)^{-2/3}, \quad (4)$$

where $\alpha_T \sim 10^{-4}$ K⁻¹ is the coefficient of thermal expansion of ice, $\Delta T_i \sim 20$ K is the approximate magnitude of temperature variations driving convection in Pluto’s core, g is the local acceleration of gravity on Pluto, and η_o is the viscosity of ice in Pluto’s deep interior (Barr and Canup, 2008). A lower limit on the time scale for the onset of convection $t_o \sim 2$ Myr can be obtained using the melting point viscosity of ice I, $\eta_o = 10^{14}$ Pa s, and Pluto’s surface gravity $g = 0.65$ m/s². Because t_o is comparable to the half-lives of ^{26}Al and ^{60}Fe , it would be difficult for Pluto to remove internal heat from these sources before they could drive internal melting. Once differentiation had begun inside Pluto, it would have become an energetically self-sustaining process, driving itself to completion. This is because the grav-

itational potential energy per unit mass associated with the differentiation of Pluto (Friedson and Stevenson, 1983; Barr and Canup, 2010),

$$E_{gr} = \frac{3}{5} \frac{GM}{R_p} \left[1 - z_1^2 x^5 - z_2^2 (1 - x^5) - \frac{5}{2} x^3 z_2 (z_1 - z_2) (1 - x^2) \right] \quad (5)$$

where $z_1 = \rho_r/\bar{\rho}$, $z_2 = \rho_i/\bar{\rho}$, $x = \phi^{1/3}$, and $E_{gr} \sim 5 \times 10^5$ J/kg, is larger than the latent heat of water ice.

We also consider it likely that Pluto had an ocean post-impact, and that the ocean may persist even to the present day. Assuming an equilibrium between present chondritic heat flow and the convective heat flux, Pluto could be warm enough to harbor an ocean beneath > 100 km of ice (Hussmann et al., 2006). Variations in ice shell thickness can lead to stresses that differ by a factor of ~ 2 from estimates here. However, we seek estimates of stress at an order of magnitude level, so we do not explore the effect of shell thickness variations here. Thicker oceans are possible in the past, when the chondritic heat flux was higher, and if some kind of low-eutectic material (such as ammonia) is mixed in with Pluto’s ices (Hussmann et al., 2006). Of course, as Charon’s orbital evolution results in tidal heating inside Pluto, the combination of impact induced heat, radiogenic heat, and tidal heat is likely to drive melting, which creates an ocean and could trigger runaway differentiation if Pluto were undifferentiated before. Although these simple arguments favor a differentiated Pluto with an ocean, we additionally explore cases for Pluto evolving with no ocean, and with a uniform-density interior, because they are both permitted by the impact simulations (Canup, 2005, 2011).

3.2. Love Numbers

As described in Section 2, the orbital evolution time scale for the system is strongly dependent on the Q of Pluto, which expresses the fraction of orbital energy dissipated during each diurnal tidal cycle. Previous studies have considered $Q = 100$ (e.g., Dobrovolskis et al. 1997), a value commonly assumed for icy satellites (Murray and Dermott, 1999). Models of the tidal deformation of Europa and Enceladus (Ross and Schubert, 1989; Moore and Schubert, 2000; Wahr et al., 2006) show that the values of k_2 and Q for a mixed ice/rock body depend on the degree of differentiation and whether the object has an ocean decoupling its outer ice shell from its deeper interior. Thus, the time scale for system evolution and the potential for generating tidally induced tectonics on Pluto depend strongly on its post-impact interior structure.

We estimate Q by determining how the interior of a spherically symmetric viscoelastic Pluto deforms in response to a tidal bulge raised due to Charon on a frequency ω_{tidal} . We use numerical techniques to calculate k_2 using the correspondence principle, an approach has been used to study tidal heating in rocky and icy bodies including Io, Europa, and Enceladus (Segatz et al., 1988; Ross and Schubert, 1989; Moore and Schubert, 2000; Wahr et al., 2006; Nimmo et al., 2007; Barr, 2008; Wahr et al., 2009). Details regarding the particular methods we employ, namely the portion of *Sat-Stress* that calculates Love numbers for viscoelastic planetary bodies, may be found in Wahr et al. (2009). In this approach, the response of a spherically symmetric viscoelastic planet to an applied tidal potential with varying harmonic degree is calculated as a function of the tidal frequency and material

properties of the planet.

For a viscoelastic body, k_2 can be considered a complex number (which we denote k_2^*), where the real part of k_2^* , $Re(k_2^*)$, is related to elastic (recoverable, adiabatic) deformation occurring over a time scale $2\pi/\omega_{tidal}$, and the imaginary part, $Im(k_2^*)$, is related to the non-recoverable dissipation occurring inside Pluto over the tidal time scale (Segatz et al., 1988; Wahr et al., 2009). The tidal quality factor is related to k_2^* (Segatz et al., 1988),

$$Q = \frac{|k_2^*|}{Im(k_2^*)}, \quad (6)$$

which allows us to substitute $1/Im(k_2^*)$ for the ratio Q/k_2 in equation (2).

3.2.1. Interior States

For a differentiated Pluto with an ocean (Figure 2a), we consider an elastic rocky core and an overlying viscoelastic ice shell. The values of Young's modulus and Poisson's ratio for rock are summarized in Table 2. We use an ice shell with a thickness of 100 km (Hussmann et al., 2006) and an upper layer of cold rigid ice 15 km thick, to represent the cold lithosphere atop the warm sublayer of a convecting ice shell. We assume a Newtonian volume diffusion rheology for ice, appropriate for deformation at low stresses (Goldsby and Kohlstedt, 2001; Barr and McKinnon, 2007). The viscosity varies as a function of temperature as (Goldsby and Kohlstedt, 2001),

$$\eta(T) = \frac{3R_G T d^2}{14V_m D_{o,v}} \exp\left(\frac{Q^*}{R_G T}\right) \quad (7)$$

with gas constant $R_G = 8.314$ J/mol-K, molar volume $V_m = 1.95 \times 10^{-5}$ m³/mol, diffusion constant $D_{o,v} = 9.10 \times 10^{-4}$ m²/s, and activation energy $Q^* = 59.4$ kJ/mol. The viscosity is strongly dependent on ice grain size, d .

Given the low stresses associated with flow in the interior of Pluto, and the likely presence of small silicate particles mixed in its ices, the grain size in Pluto’s interior is plausibly $d \sim 0.1$ to 1 mm (Barr and McKinnon, 2007). This yields a melting point viscosity for water ice of $\eta = 5 \times 10^{14} (d/0.3 \text{ mm})^2$ Pa s, or $\eta \sim 6 \times 10^{13}$ Pa s for $d = 0.1$ mm, close to the lower limit of what could be expected in natural systems (Barr and McKinnon, 2007). To explore the full range of possible values of ice viscosity, we vary the viscosity of the lower ice layer from 6×10^{13} Pa s to 10^{20} Pa s. We consider 10^{20} Pa s a plausible upper limit for the “bulk” viscosity of a convective or conductive ice shell on Pluto, corresponding to the viscosity of ice at $T \sim 200$ K. The cold ice “lithosphere” has a constant viscosity of 10^{24} Pa s, corresponding to a mean temperature $T \sim 150$ K. The ocean is represented by a fluid layer with a density $\rho_w = 1000 \text{ kg/m}^3$.

The interior state for a differentiated Pluto without an ocean (Figure 2b) is similar to the differentiated case (see Table 2), but without the fluid layer. We only consider a single ice layer in this case, to obtain upper limits on the value of k_2^* and a lower limit on Q and thus the timescale for orbital evolution for Charon. If we added a near-surface layer of cold ice with $\eta \sim 10^{24}$ Pa s, this would only serve to decrease k_2^* .

For a uniform-density Pluto, we assume that the interior consists of a convecting homogeneous ice/rock mixture with a constant viscosity, overlain by a 15 kilometer thick ice “lithosphere.” We assume that the mixture of ice and rock in the convecting sublayer has a Young’s modulus and Poisson’s ratio similar to those for pure water ice. The viscosity of the sublayer is varied from 6×10^{13} Pa s to 10^{20} Pa s. The viscosity of ice with up to ~ 40

to 50% silicate by volume is only a factor of ~ 2 higher than the viscosity of pure water ice (Friedson and Stevenson, 1983; Durham et al., 1992).

3.2.2. Tidal Frequency

Because angular momentum is conserved during the orbital evolution of the system, the present total angular momentum of the system can be used to relate Pluto's initial spin frequency, ω_p , to the initial semi-major axis of Charon's orbit, a_o . The total angular momentum of the present system is the sum of the orbital angular momentum of Charon and the spin angular momentum of each body, $L_{tot} = L_{orbital} + L_{spin,p} + L_{spin,c}$, where $L_{orbital} = n_f a^2 (m_p m_c) / (m_p + m_c)$ and $L_{spin} = \alpha m r^2 \omega$, where α is the moment of inertia coefficient, $\alpha = C / m r^2$, and $\omega = n_f$ because Pluto's spin frequency, Charon's spin frequency, and Charon's orbital frequency are presently equal. The angular momentum immediately following the impact has a similar form, with $\omega_c = n_o = (G m_p / a_o^3)^{1/2}$ with a_o as a free parameter.

Equating the present angular momentum equal to that immediately post-impact, we obtain a relationship between the spin frequency of Pluto post-impact, Charon's initial orbital semi-major axis, and the current dynamical state of the system,

$$\frac{\omega_p}{n_f} = 1 + \frac{m_c}{\alpha_p (m_p + m_c)} \left[\left(\frac{a_f}{r_p} \right)^2 - \left(\frac{a_o}{r_p} \right)^2 \left(\frac{n_o}{n_f} \right) \right] + \frac{\alpha_c m_c}{\alpha_p m_p} \left(\frac{r_c}{r_p} \right)^2 \left(1 - \frac{n_o}{n_f} \right). \quad (8)$$

The initial tidal frequency $\omega_{tidal} = \omega_p - n_o$. We calculate k_2^* for Pluto for every value of a_o from $3.7 r_p$ to $21 r_p$, in increments of $0.1 r_p$, for mean interior viscosity values from $\sim 6 \times 10^{13}$ to 10^{20} Pa s, in five logarithmically spaced increments for each order of magnitude.

The moment of inertia coefficient (α) for each body is (Friedson and Stevenson,

1983),

$$\alpha = \frac{2}{5} \frac{1}{\bar{\rho}} \left[\rho_i (1 - x^5) + \rho_r x^5 \right], \quad (9)$$

where x is the fractional radius of the rock core in each body. When Pluto is fully differentiated, we assume that Charon is as well; for uniform-density plutos, we assume that Charon is undifferentiated.

3.3. *Orbital Evolution Due to Pluto Tides*

For each combination of interior structure and k_2^* calculated from a_o and mean interior viscosity, equation (2) can be used to determine the time it takes for Charon's orbit to move by $0.1 r_p$, which is the spacing between successive calculations of k_2^* in section 3.2. We then integrate equation (2) for all Charon starting distances and Pluto viscosities by summing the time spent at all intermediate stages from a_o to a_f .

3.4. *Thermal Evolution of Pluto*

Although the total amount of tidal energy dissipated during the orbital evolution is modest (Dobrovolskis et al., 1997), the heat *flux* through the ice shell could be substantial, particularly if the orbital evolution time scale is short. The average energy dissipation rate within Pluto over the time period of orbital evolution is the sum of the change in Pluto's rotational energy and the system orbital energy, as angular momentum is conserved. If eccentricity is zero, the energy dissipation rate within Pluto is

$$\frac{dE_p}{dt} = \frac{1}{2} \left(\omega_p m_c \sqrt{\frac{Gm_p}{a}} + \frac{Gm_p m_c}{a^2} \right) \frac{da_p}{dt}, \quad (10)$$

(Mignard, 1980). If this energy was instantly converted into heat flowing out of Pluto's surface, the tidal heat flow, $F = (dE_p/dt)/(4\pi R_p^2)$.

We can construct a basic understanding of the response of Pluto's interior to the tidal heat by comparing the heat flux from tidal dissipation to the heat flux from conduction and solid-state convection. Solid-state convection will occur in Pluto's interior (or in its outer ice I shell, in the case of a differentiated body) if the Rayleigh number of the convecting layer,

$$Ra = \frac{\rho g \alpha_T \Delta T D^3}{\kappa \eta(T_i)}, \quad (11)$$

exceeds a critical value. Here, T_i is the temperature in the warm convecting sublayer of the ice shell, D is the ice shell thickness, $\Delta T = T_i - T_s$ where $T_s \sim 40$ K is the surface temperature on Pluto, $g = 0.65$ m/s² is the surface gravity, $\alpha_T = 1.56 \times 10^{-4} (T_i/250 \text{ K}) \text{ K}^{-1}$, $\kappa = 1.47 \times 10^{-6} (250 \text{ K}/T_i)^2 \text{ m s}^{-2}$ is the thermal diffusivity (Kirk and Stevenson, 1987). The critical Rayleigh number for convection in a Newtonian fluid with strongly temperature-dependent viscosity, $Ra_{cr} = 20.9\theta^4$ (Solomatov, 1995), where $\theta \approx Q^* \Delta T / (R_G T_i^2)$, and T_i is the temperature in the warm convecting sub-layer of the ice shell. The value of T_i is calculated from the effective interior viscosity of the ice shell, η_i by solving equation (7) for T . For a uniform density pluto, $D \sim 300$ km, a rough estimate of the depth at which the lithostatic pressure exceeds 209 MPa, the location of the ice I/III phase boundary (Hobbs, 1974). For a differentiated Pluto, $D = 230$ km if there is no ocean, and $D = 100$ km if there is an ocean (see Table 2).

If convection occurs, the heat flow, $F_{conv} = \frac{k \Delta T}{D} Nu$, where Nu is the Nusselt number, which describes the efficiency of convective heat transport relative to conductive transport alone. For a Newtonian fluid with a strongly temperature dependent viscosity, $Nu \approx 0.53\theta^{-4/3} Ra^{1/3}$ (Solomatov and Moresi, 2000). Evaluating Ra , θ , and Nu gives an estimate for the convective heat

flux,

$$F_{conv} = 0.53 \left(\frac{Q^*}{R_G T_i^2} \right)^{-4/3} \left(\frac{\rho g \alpha_T k^3}{\kappa \eta (T_i)} \right)^{1/3}, \quad (12)$$

which notably, does not depend on the thickness of the convecting layer (D).

If the viscosity of the ice shell is too high to permit convection, we compare the tidal heat flux to the heat flux that could be carried by conduction alone,

$$F_{cond} = \frac{k \Delta T}{D}, \quad (13)$$

where we assume a constant thermal conductivity for the shell, $k = 651/T_{ave}$ W m⁻¹ K⁻¹ (Petrenko and Whitworth, 1999), and $T_{ave} = T_s + \Delta T/2$. The net heat flux across the ice shell, $F_{net} = F - F_{cond,conv}$ is used to give a rough idea about whether the ice shell would melt or thicken during tidal evolution; $F_{net} > 0$ implies melting, and $F_{net} < 0$ implies thickening. Values of viscosity where $F_{net} = 0$ are locations where the ice shell is in thermodynamic equilibrium with the tidal dissipation rate averaged over the entire orbital evolution. Because the tidal heat flux will vary over the course of the orbital evolution, these represent only speculative stable states.

3.5. Surface Stress Due to Orbital Evolution

Orbital evolution in the Pluto/Charon system drives Charon's orbital radius from its starting point to a distance of 16.4 r_p while changing the spin rate of Pluto. These changes in turn change the equilibrium figures of Pluto and Charon, which in turn induce stress on their surfaces. Whether the induced stress causes the formation of tectonic features on the surfaces of these two bodies depends on the magnitude of the figure change and the rate of stress buildup versus viscous relaxation.

Over the time period of orbital evolution, Pluto’s spin rate changes from $\omega_{p,o}$ to $\omega_{p,f}$. The change in equilibrium spin flattening of Pluto changes by

$$\Delta f = \frac{h_2 r_p^3}{2Gm_p} (\omega_{p,o}^2 - \omega_{p,f}^2) \quad (14)$$

where h_2 is a Love number, which we use at its maximum value of 5/2 to obtain a maximum stress estimate. Somewhat lower values of h_2 are likely due to more rigid behavior of Pluto or Charon, and would modify the stress calculated below by a factor of $2h_2/5$. If the rigidity of Pluto’s lithosphere at the hemispherical scale over the time period of orbital evolution is negligible, it will behave as a thin elastic shell. Melosh (1977) described stresses in a thin elastic shell undergoing despinning, and Matsuyama and Nimmo (2008) derived equivalent stress equations (with the sign of the stress reversed and using a different trigonometric identity). Here we describe stresses using the positive compression convention. Based on the work of Melosh (1977) and Matsuyama and Nimmo (2008), the stresses due to despinning may be represented as

$$\sigma_{radial} = -\frac{\Delta f}{3} \mu \left(\frac{1+\nu}{5+\nu} \right) (5 - 3 \cos 2\lambda) \quad (15)$$

for stresses oriented north-south (radial to the spin axis) and

$$\sigma_{tangential} = \frac{\Delta f}{3} \mu \left(\frac{1+\nu}{5+\nu} \right) (1 + 9 \cos 2\lambda) \quad (16)$$

for stresses oriented east-west (tangential to the spin axis), where λ is latitude, μ is the shear modulus, and ν is Poisson’s ratio.

After it becomes tidally locked, Charon no longer experiences pure despinning, but instead its tidal and rotational equilibrium distortions simultaneously change as a function of distance from Pluto. This stress scenario was

described by Melosh (1980), Helfenstein and Parmentier (1983), and more recently by Matsuyama and Nimmo (2008). The underlying equations are the same as (15) and (16), but the distortion of the body now has two components that can be linearly superposed: the oblate flattening around the spin axis, and the prolate flattening around the tidal axis. Because the magnitude of the tidal and rotational distortions necessarily change together with orbital distance in a tidally locked body, the change in tidal flattening is always -3 times the change in spin flattening (cf. Melosh 1980; Matsuyama and Nimmo 2008). Therefore, the stress at any point can be calculated by first determining the despinning stress using (15) and (16), and then calculating the same stress, multiplied by -3, oriented radial and tangential to the tidal axis instead of the spin pole.

For both Pluto and Charon in each orbital evolution scenario, the maximum compressional stress σ_c and tensile stress σ_t anywhere on the surface is calculated. This is a maximum stress estimate, as it assumes that each body changed shape to match its equilibrium figure (negligible rigidity), and it assumes that all of the stress due to orbital evolution was able to accumulate without relaxing away. Like most geological materials, ice is weakest in tension, and the tensile strength of ice near Pluto's surface temperature of 40 K should be approximately 2.5 MPa (Litwin et al., 2012). This is significantly higher than the yield strength for ice failing along pre-existing fractures (Beeman et al., 1988) and so our choice represents a conservative value and failure in a pre-fractured lithosphere could take place at stresses an order of magnitude lower. If the maximum tensile stress on Pluto or Charon in a given orbital evolution scenario does not reach this value, we consider

this case to represent “unlikely tectonic activity.” If the maximum tensile stress is above this value, tectonic activity may be possible.

To refine this assessment, we examine the rate of stress buildup over time. We calculate the Maxwell viscoelastic relaxation of stress over the entire timescale of orbital evolution τ to determine the residual stress

$$\sigma_{ve} = \sigma_{c,t} e^{-\frac{E\tau}{2\mu_{lid}}} \quad (17)$$

where E is Young’s modulus and μ_{lid} is the viscosity of the cold near-surface ice. If the residual stress is still above 2.5 MPa after viscous relaxation over the orbital evolution time period, we consider the case to represent “likely tectonic activity.”

4. Results

4.1. Differentiated, No Ocean

Figure 3a illustrates the time scale for Charon to evolve from the synchronous to dual synchronous state, for the case where Pluto does not initially have an ocean (interior state depicted in Figure 2b). The time scale for evolution is a strong function of the viscosity of the ice shell and ranges from $\sim 10^4$ years to much longer than ~ 4.5 Gyr, the age of the solar system. (Orbital evolution timescales longer than the age of the solar system are obviously not tenable, and so are represented as a gray shade on Figure 3 and subsequent figures). The evolution times for this interior model are extremely long because Pluto’s ice shell is rigidly coupled to its rock core, preventing significant tidal deformation and slowing the rate at which angular momentum is transferred between the two bodies (see equation 1). We

find that if Charon starts far from the dual-synchronous point ($a_o/R_p < 15$ or $a_o/R_p > 19$), Pluto must be warmed close to its melting point in order for Charon’s orbit to evolve in $t_{evol} < 4.5$ Gyr. Pluto’s ice shell must have an interior viscosity less than 2×10^{15} Pa s, equal to the viscosity of ice at $T = 239$ K for $d = 0.1$ mm, the lowest grain size that could be expected in the ice shell (Barr and McKinnon, 2007). Assuming a more realistic $d = 0.3$ mm, this viscosity is achieved only at $T = 258$ K, very close to the melting point of ice. Such a low viscosity allows enough deformation in the ice shell to permit Charon’s orbit to evolve, albeit slowly. If Charon starts close to the synchronous point ($15 \lesssim a_o/R_p \lesssim 19$), evolution times shorter than the age of the solar system are possible for viscosities up to 1.5×10^{17} Pa s, corresponding to interior temperatures $T \sim 210$ K for the minimum grain size of 0.1 mm, or $T \sim 225$ K for $d = 0.3$ mm.

Figure 3b illustrates the heat flux from tidal dissipation, averaged over Charon’s orbital evolution. We find that the heat flows range from $F = 10^{-3}$ to ~ 100 mW m $^{-2}$, although the vast majority of orbital scenarios give heat flows of order tens of milliwatts per meter squared. For the vast majority of orbital evolution scenarios and interior viscosities, the amount of tidal heat deposited in Pluto’s ice shell will be small enough to allow Pluto to remain solid (and avoid forming an ocean) during Charon’s orbital evolution.

Figures 3c and 3d illustrate the maximum stresses on the surface of Pluto during the orbital evolution. The maximum stress achieved is large $\sigma_{max} = 340$ MPa, but decreases as a function of a_o/R_p . Tectonic activity is “likely” on Pluto (as defined at the end of section 3.5) only if the ice shell has a very low viscosity $\eta_i < 2 \times 10^{14}$ Pa s and $a_o/R_p < 15.2$ or $a_o/R_p > 18.2$.

Thus, we consider it likely that Charon can evolve into the dual synchronous state even if Pluto does not have an ocean and its outer ice shell is mechanically coupled to its much stiffer rock core. However, Pluto will only display evidence of ancient tectonic resurfacing if its interior viscosity is quite low, corresponding to a warm ice shell. For $a_o/R_p \sim 3.4$ to 10, model plutos with very warm ice shells could likely experience runaway melting from tides, leading to the formation of an ocean. For $a_o \sim 10$ to 15.2, a warm ice shell on Pluto can be tectonically active without melting from tidal dissipation.

4.2. Undifferentiated

Figure 4 illustrates our results for an undifferentiated Pluto. Here, the entire interior of Pluto has a rheology appropriate for water ice, which allows it to experience more tidal deformation and dissipation than a differentiated model pluto without an ocean whose ice shell is rigidly coupled to its rocky core. We find that an undifferentiated Pluto/Charon system can reach the dual synchronous state in a time scale less than the age of the solar system if its interior viscosity is less than 10^{19} Pa s, or $T = 173$ K for $d = 0.1$ mm, or $T = 198$ K for $d = 0.3$ mm (see Figure 4a).

An undifferentiated Pluto experiences significantly more tidal dissipation than its differentiated counterpart, even if it never has an ocean. Figure 4b shows the estimated tidal heat fluxes, and the range of interior viscosities that permit freezing or melting of the ice shell. Initially high-viscosity (cold) shells will remain cold and could thicken. Ice shells that are initially warm, with $\eta_i < 10^{16}$ to 10^{17} Pa s, or $T \sim 200$ to 230 K, depending on grain size, will experience strong tidal dissipation in excess of the amount that could be removed by conduction and/or convection, which could lead to melting.

Because runaway differentiation may be possible in Pluto (see Section 3.1), we consider that the onset of melting would trigger complete differentiation of the body in addition to thickening of the outer ice shell and formation of an ocean; the interior state of Pluto evolves to that depicted in Figure 2a. Once the ice shell began to melt, the amount of tidal dissipation would decrease since the thickness of the shell had decreased (Cassen et al., 1979, 1980). Eventually an equilibrium between tidal heat and conductive/convective heat transport may be achieved (e.g., Moore 2006).

The maximum stress experienced is $\sigma_{max} \sim 250$ MPa, far in excess of the strength of water ice. Tectonic activity is “likely” on Pluto if its ice shell has a viscosity $\eta_i < 7 \times 10^{16}$ Pa s and $a_o/R_p < 15$ or $a_o/R_p > 18.6$. Because this viscosity is associated with tidal dissipation that would lead to melting, an undifferentiated Pluto is incompatible with tidally-driven tectonic activity.

4.3. *Differentiated, With Ocean*

Figure 5 illustrates the evolution time scale, heat flux, and stresses in Pluto during Charon’s orbital evolution, assuming that Pluto is fully differentiated and has a liquid water ocean. Similar to the undifferentiated case, the orbital evolution time scale is less than the age of the solar system if $\eta_i < 10^{19}$ Pa s. Tidal heat can be removed by conduction and/or convection if $\eta_i \sim 10^{16}$ to 10^{18} Pa s, roughly corresponding to $T \sim 200$ to 245 K. The presence of a subsurface ocean permits stresses $\sigma_{max} \sim 350$ MPa. Tectonic activity is “likely” on Pluto if its ice shell has a viscosity $\eta_i < 8 \times 10^{16}$ Pa s and $a_o/R_p < 15.2$ or $a_o/R_p > 18.2$.

4.4. Stress on Charon

Stress due to synchronized lowering of tidal and rotational bulges (tidal recession) was calculated on Charon for each Pluto scenario discussed above. Theoretical maximum tensile stress on Charon due to tidal recession is $\sigma_{max} \sim 250$ MPa, though the thin elastic shell assumption may be less valid for Charon than for Pluto, as Charon is not strongly heated. Tectonic activity is “likely” on Charon for $a_o/R_p < 13.4$ and for the same ranges of Pluto’s interior viscosity that made activity likely on Pluto for any of the three interior models. This is because it is Pluto’s interior that controls the rate of orbital evolution, and thus the rate of stress accumulation versus viscous relaxation.

5. Discussion

The *New Horizons* mission has sparked new interest about the thermal evolution of Pluto and its moon Charon, in particular, the possibility of tectonic resurfacing on both bodies and the likelihood that these bodies may have had liquid water oceans, either now or in the past. In this work, we have used simple tidal models to calculate the magnitude of stresses expected on the surfaces of Pluto and Charon during their evolution into the dual-synchronous state. During this time, Pluto de-spins as Charon recedes from Pluto, potentially leading to enormous stresses on the lithospheres of both bodies.

We conclude that if *New Horizons* uncovers evidence for ancient tectonic activity consistent with despinning on Pluto and/or tidal recession on Charon, the most self-consistent explanation is that Pluto had an ocean during the time period of Charon’s orbital evolution. Despinning stresses on

Pluto would manifest as normal faults at the poles, strike-slip features in the mid-latitudes, and equatorial thrust faults (Melosh, 1977). Stresses on Charon arising from the collapse of its tidal bulge would create normal faults at the poles, strike-slip faults in the mid-latitudes, with a zone of thrust faults at the sub-Pluto point (Melosh, 1980). Concurrent volume changes in the interiors of Pluto or Charon could add to these predicted stress states and significantly shift the boundaries of the tectonic regions toward or away from the poles or tidal axis. If *no* tectonic features are observed, this could indicate an extremely cold Pluto pre- or post-impact (and thus a very long timescale for orbital evolution), or that tectonic features had been removed or buried by other processes. Tectonic features formed by the post-impact evolution could have been obscured by, e.g., later flooding by cryomagmas. It is also possible that infall of Pluto’s tenuous atmosphere may subdue landforms created by ancient tectonics.

We find that the orbital evolution time scale for Charon depends sensitively on the interior thermal state of Pluto. This is because the tidal quality factor of Pluto, which controls the rate at which angular momentum is transferred from Pluto’s spin to Charon’s orbit, depends on Q , which in turn depends on the viscosity of its interior. A cold, highly viscous (“stiff”) Pluto will shed angular momentum more slowly than a warm, low-viscosity Pluto. If Pluto is differentiated and has a liquid water ocean, its ice shell is no longer rigidly coupled to its rock core, permitting large tidal deformations and rapid tidal evolution even if the ice shell has a high viscosity. For Charon to evolve to the dual synchronous state on a time scale less than the age of the solar system, a fully differentiated Pluto with an ocean (Figure 5)

must be warmed post-impact to a temperature $T \gtrsim 170$ to 190 K, so that the viscosity of the convecting portion of its ice shell, $\eta_i < 10^{19}$ Pa s. Similar conditions must be achieved in an undifferentiated Pluto. However, we consider it likely that Pluto is differentiated either before or during Charon’s tidal evolution because the energy liberated during accretion is sufficient to melt its ice, Pluto is unstable to runaway differentiation, and its high mean density implies a high rock fraction in the interior and thus, ample radiogenic heat. If Pluto did not have an ocean during Charon’s orbital evolution, its interior must be warmed to ~ 240 to 260 K for Pluto and Charon to evolve to the dual synchronous state. Temperatures this high would lead to melting, particularly if Pluto has even just a small amount of ammonia or low-eutectic salt mixed in with its ices.

While it is possible for orbital evolution to drive tectonics on Pluto and Charon for any of the assumed interior models for Pluto, the thermal/orbital pathway of the system depends sensitively on the interior states of Pluto and Charon, which may change over time. For example, in the differentiated model without an ocean, tectonics can only occur if Charon starts close to its current location, and Pluto’s ice is very close to the melting point (but not molten). In the undifferentiated model, tectonic activity occurs if the ice has a low viscosity, but this same low viscosity ice will dissipate enough heat to begin melting and possibly trigger runaway differentiation. In the differentiated Pluto model with an interior ocean, tectonic activity occurs above an interior that has the right viscosity for a floating, conducting or convecting ice shell. Thus, more detailed calculations (e.g., Robuchon and Nimmo 2011) will be warranted once the *New Horizons* mission has returned its data.

Acknowledgements

Author Barr acknowledges support from OPR NNX12AL22G. We thank R. M. Canup, R. T. Pappalardo, and S. A. Stern for helpful discussions.

References

- Ahrens, T. J., O'Keefe, J. D., 1977. Equations of state and impact-induced shock-wave attenuation on the moon. In: *Impact and Explosion Cratering*. Pergamon Press, New York, pp. 639–656.
- Barr, A. C., 2008. Mobile lid convection beneath Enceladus' south polar terrain. *Journal of Geophysical Research* 113.
- Barr, A. C., Canup, R. M., 2008. Constraints on gas giant satellite formation from the interior states of partially differentiated satellites. *Icarus* 198, 163–177.
- Barr, A. C., Canup, R. M., 2010. Origin of the Ganymede–Callisto dichotomy by impacts during the late heavy bombardment. *Nature Geoscience* 3, 164–167.
- Barr, A. C., McKinnon, W. B., 2007. Convection in ice I shells and mantles with self-consistent grain size. *J. Geophys. Res.* 112.
- Beeman, M., Durham, W. B., Kirby, S. H., 1988. Friction of Ice. *J. Geophys. Res.* 93, 7625–7633.
- Bizzarro, M., Baker, J. A., Haack, H., Lundgaard, K. L., 2005. Rapid Timescales for Accretion and Melting of Differentiated Planetsimals inferred from ^{26}Al – ^{26}Mg Chronometry. *Astrophys. J. Lett.* 632, L41–L44.
- Brown, M. E., Calvin, W. M., Jan. 2000. Evidence for Crystalline Water and Ammonia Ices on Pluto's Satellite Charon. *Science* 287, 107–109.

- Buie, M. W., Grundy, W. M., Dec. 2000. The Distribution and Physical State of H₂O on Charon. *Icarus* 148, 324–339.
- Buie, M. W., Grundy, W. M., Young, E. F., Young, L. A., Stern, S. A., 2006. Orbits and photometry of Pluto’s satellites: Charon, S/2005 P1, and S/2005 P2. *The Astronomical Journal* 132 (1), 290.
- Canup, R. M., Jan. 2005. A Giant Impact Origin of Pluto-Charon. *Science* 307, 546–550.
- Canup, R. M., 2008. Personal Communication.
- Canup, R. M., 2011. On a giant impact origin of Charon, Nix, and Hydra. *The Astronomical Journal* 141 (2), 35.
- Cassen, P., Peale, S. J., Reynolds, R. T., Nov. 1980. Tidal dissipation in Europa - A correction. *Geophys. Res. Lett.* 7, 987–988.
- Cassen, P., Reynolds, R. T., Peale, S. J., Sep. 1979. Is there liquid water on Europa. *Geophys. Res. Lett.* 6, 731–734.
- Collins, G. C., Pappalardo, R. T., Mar. 2000. Predicted Stress Patterns on Pluto and Charon due to their Mutual Orbital Evolution, abstract no. 1035. In: *Lunar and Planet. Sci. Conf. Abstracts XXXI*. Lunar and Planetary Institute, Houston, Tex.
- Cook, J. C., Desch, S. J., Roush, T. L., Trujillo, C. A., Geballe, T. R., Jul. 2007. Near-Infrared Spectroscopy of Charon: Possible Evidence for Cryovolcanism on Kuiper Belt Objects. *Astrophys. J.* 663, 1406–1419.

- Dobrovolskis, A. R., Peale, S. J., Harris, A. W., 1997. Dynamics of the Pluto-Charon Binary. In: Burns, J. A., Matthews, M. S. (Eds.), *Pluto and Charon*. University of Arizona Press, Tucson, AZ, pp. 159–190.
- Durham, W. B., Kirby, S. H., Stern, L. A., 1992. Effects of Dispersed Particulates on the Rheology of Water Ice at Planetary Conditions. *J. Geophys. Res.* 97, 20,883–20,897.
- Friedson, A. J., Stevenson, D. J., Oct. 1983. Viscosity of rock-ice mixtures and applications to the evolution of icy satellites. *Icarus* 56, 1–14.
- Goldsby, D. L., Kohlstedt, D. L., Jun. 2001. Superplastic deformation of ice: Experimental observations. *J. Geophys. Res.* 106, 11017–11030.
- Greeley, R. C., Chyba, C., Head, J. W., McCord, T., McKinnon, W. B., Pappalardo, R. T., 2004. Geology of Europa. In: *Jupiter: The Planet, Satellites & Magnetosphere*. Cambridge University Press, New York, pp. 329–362.
- Gulbis, A. A. S., Ellito, J. L., Person, M. J., Adams, E. R., Babcock, B. A., Emilio, M., Gangestad, J. W., Kern, S. D., Kramer, E. A., Osip, D. J., Pasachoff, J. M., Souza, S. P., Tuvikene, T., 2006. Charon’s radius and atmospheric constraints from observations of a stellar occultation. *Nature* 439, 48–50.
- Haisch, Jr., K. E., Lada, E. A., Lada, C. J., 2001. Disk Frequencies and Lifetimes in Young Clusters. *Astrophys. J. Lett.* 553, L153–L156.
- Helfenstein, P., Parmentier, E. M., 1983. Patterns of fracture and tidal stresses on Europa. *Icarus* 53, 415–430.

- Hobbs, P. V., 1974. Ice physics. Oxford: Clarendon Press.
- Hoppa, G. V., Tufts, B. R., Greenberg, R., Geissler, P. E., 1999. Formation of cycloidal features on Europa. *Icarus* 141, 287–298.
- Hurford, T. A., Sarid, A. R., Greenberg, R., 2007. Cycloidal cracks on Europa: Improved modeling and non-synchronous rotation implications. *Icarus* 186, 218–233.
- Husmann, H., Sohl, F., Spohn, T., 2006. Subsurface oceans and deep interiors of medium-sized outer planet satellites and large trans-neptunian objects. *Icarus* 185, 258–273.
- Kehle, R. O., 1964. Deformation of the Ross Ice Shelf. *Geol. Soc. Amer. Bull* 75, 259–286.
- Kenyon, S. J., Bromley, B. C., 2014. The formation of Pluto’s low mass satellites. *Astrophys. J.* 147, 8.
- Kirk, R. L., Stevenson, D. J., Jan. 1987. Thermal evolution of a differentiated Ganymede and implications for surface features. *Icarus* 69, 91–134.
- Litwin, K. L., Zygielbaum, B. R., Polito, P. J., Sklar, L. S., Collins, G. C., 2012. Influence of temperature, composition, and grain size on the tensile failure of water ice: Implications for erosion on titan. *Journal of Geophysical Research* 117 (E8), 10.1029/2012JE004101.
- Lodders, K., Jul. 2003. Solar system abundances and condensation temperatures of the elements. *Astrophys. J.* 591, 1220–1247.

- Love, A. E. H., 1944. A Treatise on the Mathematical Theory of Elasticity. Dover Publications, New York.
- Matsuyama, I., Nimmo, F., 2008. Tectonic patterns on reoriented and despun planetary bodies. *Icarus* 195, 459–473.
- McKinnon, W. B., Prialnik, D., Stern, S. A., Coradini, A., 2008. Structure and Evolution of Kuiper Belt Objects and Dwarf Planets. In: Barucci, M., Boehnhardt, M., Cruikshank, D. P., Morbidelli, A. (Eds.), *The Solar System Beyond Neptune*. University of Arizona Press and the Lunar and Planetary Institute, Tucson, AZ, pp. 213–242.
- McKinnon, W. B., Simonelli, D. P., Schubert, G., 1997. Composition, Internal Structure, and Thermal Evolution of Pluto and Charon. In: Burns, J. A., Matthews, M. S. (Eds.), *Pluto and Charon*. University of Arizona Press, Tucson, AZ, pp. 295–343.
- Melosh, H. J., 1977. Global tectonics of a despun planet. *Icarus* 31, 221–243.
- Melosh, H. J., 1980. Tectonic patterns on a tidally distorted planet. *Icarus* 43, 334–337.
- Mignard, F., Oct. 1980. The evolution of the lunar orbit revisited. II. *Moon and Planets* 23, 185–201.
- Moore, W. B., Jan. 2006. Thermal equilibrium in Europa’s ice shell. *Icarus* 180, 141–146.
- Moore, W. B., Schubert, G., Sep. 2000. The tidal response of Europa. *Icarus* 147, 317–319.

- Mostefaoui, S., Lugmair, G. W., Hoppe, P., El Gorse, A., 2004. Evidence for live ^{60}Fe in Meteorites. *New Astron. Reviews* 48, 155–159.
- Mueller, S., McKinnon, W. B., Dec. 1988. Three-layered models of Ganymede and Callisto - Compositions, structures, and aspects of evolution. *Icarus* 76, 437–464.
- Murray, C. D., Dermott, S. F., 1999. *Solar System Dynamics*. Cambridge University Press, New York.
- Nimmo, F., Spencer, J. R., Pappalardo, R. T., Mullen, M. E., 2007. Shear heating as the origin of plumes and heat flux on Enceladus. *Nature* 447, 289–291.
- Olkin, C. B., Wasserman, L. H., Franz, O. G., 2003. The mass ratio of Charon to Pluto from Hubble Space Telescope astrometry with the fine guidance sensors. *Icarus* 164, 254–259.
- Peale, S. J., 1986. Orbital resonances, unusual configurations, and exotic rotation states among planetary satellites. In: Burns, J. A., Matthews, M. S. (Eds.), *Satellites*. University of Arizona Press, Tucson, AZ, pp. 224–292.
- Petrenko, V. F., Whitworth, R. W., 1999. *Physics of Ice*. Oxford University Press, New York.
- Robuchon, G., Nimmo, F., 2011. Thermal evolution of Pluto and implications for surface tectonics and a subsurface ocean. *Icarus* 216, 426–439.

- Ross, M., Schubert, G., 1989. Viscoelastic models of tidal heating in Enceladus. *Icarus* 78, 90–101.
- Schubert, G., Spohn, T., Reynolds, R. T., 1986. Thermal Histories, Compositions, and Internal Structures of the Moons of the Solar System. In: Burns, J. A., Matthews, M. S. (Eds.), *Satellites*. University of Arizona Press, Tucson, AZ, pp. 224–292.
- Segatz, M., Spohn, T., Ross, M. N., Schubert, G., 1988. Tidal Dissipation, Surface Heat Flow, and Figure of Viscoelastic Models of Io. *Icarus* 75, 187–206.
- Showalter, M. R., Hamilton, D. P., Stern, S. A., Weaver, H. A., Steffl, A. J., Young, L. A., Sep. 2011. New Satellite of (134340) Pluto: S/2011 (134340) 1. IAU Circ. 9221.
- Showalter, M. R., Weaver, H. A., Buie, M. W., Hamilton, D. P., Merline, W., Mutchler, M., Steffl, A. J., Stern, S. A., H., T., Young, L. A., Jul. 2013. Orbits and Physical Properties of Pluto’s Small Moons “P4” and “P5”. In: *The Pluto system on the eve of exploration by New Horizons: Perspectives and predictions*.
- Showalter, M. R., Weaver, H. A., Stern, S. A., Steffl, A. J., Buie, M. W., Merline, W. J., Mutchler, M. J., Soummer, R., Throop, H. B., Jul. 2012. New Satellite of (134340) Pluto: S/2012 (134340) 1. IAU Circ. 9253.
- Solomatov, V. S., 1995. Scaling of temperature- and stress-dependent viscosity convection. *Physics of Fluids* 7, 266–274.

- Solomatov, V. S., Moresi, L.-N., 2000. Scaling of time-dependent stagnant lid convection: Application to small-scale convection on Earth and other terrestrial planets. *J. Geophys. Res.* 105, 21795–21818.
- Stempel, M. M., Barr, A. C., Pappalardo, R. T., 2005. Model constraints on the opening rates of bands on Europa. *Icarus* 177, 297–304.
- Stern, S., Weaver, H., Steffl, A., Mutchler, M., Merline, W., Buie, M., Young, E., Young, L., Spencer, J., 2006. A giant impact origin for Pluto’s small moons and satellite multiplicity in the Kuiper belt. *Nature* 439 (7079), 946–948.
- Tachibana, S., Huss, G. R., May 2003. The Initial Abundance of ^{60}Fe in the Solar System. *Astrophys. J. Lett.* 588, 41–44.
- Thi, W. F., Blake, G. A., van Dishoeck, E. F., van Zandelhoof, G. J., Horn, J. M. M., Becklin, E. E., Mannings, V., Sargent, A. I., van den Ancker, M. E., Natta, A., 2001. Substantial reservoirs of molecular hydrogen in the debris disks around young stars. *Nature* 409, 60–63.
- Tholen, D. J., Buie, M. W., Grundy, W. M., Elliott, G. T., Mar. 2008. Masses of Nix and Hydra. *Astron. J.* 135, 777–784.
- Thrane, K., Bizzarro, M., Baker, J. A., 2006. Brief formation interval for refractory inclusions and uniform distribution of ^{26}Al in the early solar system. *Astrophys. J.* 646, L159–L162.
- Wadhwa, M., Amelin, Y., Davis, A. M., Lugmair, G. W., Meyer, B., Gounelle, M., Desch, S. J., 2007. From Dust to Planetesimals: Implications for the Solar Protoplanetary Disk from Short-lived Radionuclides.

- In: B. Reipurth, D. Jewitt, K. K. (Ed.), *Protostars and Protoplanets V*. University of Arizona Press and the Lunar and Planetary Institute, Tucson, AZ, pp. 835–848.
- Wahr, J., Selvens, Z. A., Mullen, M. E., Barr, A. C., Collins, G. C., Selvens, M. M., Pappalardo, R. T., 2009. Modeling stresses on satellites due to non-synchronous rotation and orbital eccentricity using gravitational potential theory. *Icarus* 200 (1), 188–206.
- Wahr, J. M., Zuber, M. T., Smith, D. E., Lunine, J. I., 2006. Tides on Europa, and the thickness of Europa’s icy shell. *Journal of Geophysical Research* 111.
- Ward, W. R., Canup, R. M., 2006. Forced resonant migration of Pluto’s outer satellites by Charon. *Science* 313 (5790), 1107–1109.
- Weaver, H. A., Stern, S. A., Mutchler, M. J., Steffl, A. J., Buie, M. W., Merline, W. J., Spencer, J. R., Young, E. F., Young, L. A., Feb. 2006. Discovery of two new satellites of Pluto. *Nature* 439, 943–945.
- Zaranek, S. E., Parmentier, E. M., 2004. The onset of convection in fluids with strongly temperature-dependent viscosity cooled from above with implications for planetary lithospheres. *Earth Planet. Sci. Lett.* 224, 371–386.

Parameter	Pluto	Charon
Mass ^a	1.304×10^{22} kg	1.520×10^{21} kg
Radius ^a	1147 km	606 km
Mean Density ^a	2060 kg m ⁻³	1630 kg m ⁻³
Surface Gravity	0.66 m/s ²	0.28 m/s ²
Present Orbital Period ^a	–	6.38270 days
Present Spin Period ^a	1.139×10^{-5} s ⁻¹	1.139×10^{-5} s ⁻¹
Ice Density	1000 kg m ⁻³	1000 kg m ⁻³
Rock Density	3000 kg m ⁻³	3000 kg m ⁻³
Rock Mass Fraction	0.81	0.58
Rock Volume Fraction	0.53	0.315
Moment of Inertia Factor		
Differentiated	0.328	0.317
Undifferentiated	0.4	0.4

Table 1: Properties of the Pluto/Charon System. ^a From four-body orbital solution of Tholen et al. (2008)

Table 2: Physical and Rheological Properties of a Differentiated Pluto

Layer	Parameter	Pluto, No Ocean	Pluto With Ocean
Rocky Core	Radius	917 km	917 km
	Density	3000 kg m^{-3}	3000 kg m^{-3}
	Young's Modulus	$2.5 \times 10^{11} \text{ Pa}$	$2.5 \times 10^{11} \text{ Pa}$
	Poisson's Ratio	0.25	0.25
Ocean	Thickness	–	130 km
	Density	–	1000 kg m^{-3}
	P-Wave Velocity	–	1.45 km s^{-1}
Ice Shell	Total Thickness	230 km	100 km
	Rigid Lid Thickness	–	15 km
	Lid Viscosity	10^{24} Pa s	10^{24} Pa s
	Sublayer Thickness	219 km	85 km
	Sublayer Viscosity	variable	variable

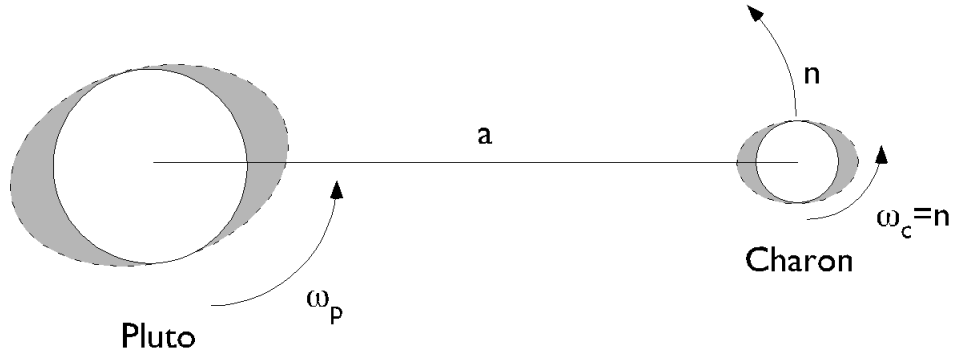


Figure 1: Schematic of the orbital state of Pluto and Charon during the system’s evolution assumed in our study. After the P/C-forming impact, Charon is launched into an eccentric orbit around Pluto, but rapidly evolves into a synchronous orbit where its spin frequency (ω_c) is equal to its orbital frequency (n). Pluto spins rapidly with frequency ω_p . The system continues to evolve over a long time scale, τ_{evol} , as the spin angular momentum of Pluto is transferred to Charon, changing its orbital semi-major axis, a . Tides are raised and lowered in Pluto with a frequency $\omega_{tidal} = \omega_p - n$. In the present-day dual synchronous state, $\omega_p = \omega_c = n = 1.13 \times 10^{-5} \text{ s}^{-1}$, and $a = 16.4R_p$.

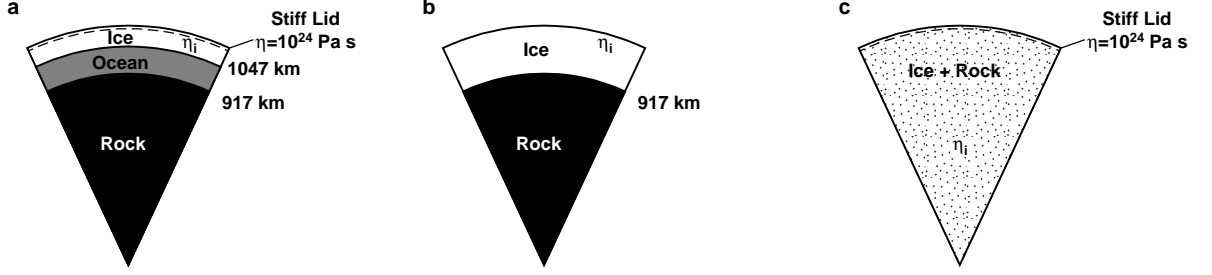


Figure 2: Interior structure models assumed for Pluto. (a) Fully differentiated with a rocky core of density $\rho_r = 3000 \text{ kg m}^{-3}$, liquid ocean of density $\rho_w = 1000 \text{ kg m}^{-3}$, and 100 kilometer thick outer ice shell with density $\rho_i = 1000 \text{ kg m}^{-3}$. The ice shell has a 15 kilometer-thick layer of stiff ice (effective viscosity $\eta = 10^{24} \text{ Pa s}$); the viscosity of the lower portion of the ice shell η_i is a key control on the amount of tidal deformation and stress experienced by Pluto during Charon's orbital evolution. The relative thickness of solid ice compared to liquid is unknown, but the amplitude of the tidal deformation is mainly controlled by the presence of the ocean, and is relatively insensitive to the thickness of the ice shell (Wahr et al., 2006). (b) Fully differentiated Pluto with no ocean, where the inner rock core is frozen to, and thus rigidly coupled to, the overlying ice shell. The viscosity of the ice shell η_i controls the amount of tidal deformation. (c) A uniform-density Pluto. The model has a stiff lid with effective viscosity $\eta = 10^{24} \text{ Pa s}$, and the viscosity of the interior η_i controls the amount of tidal deformation.

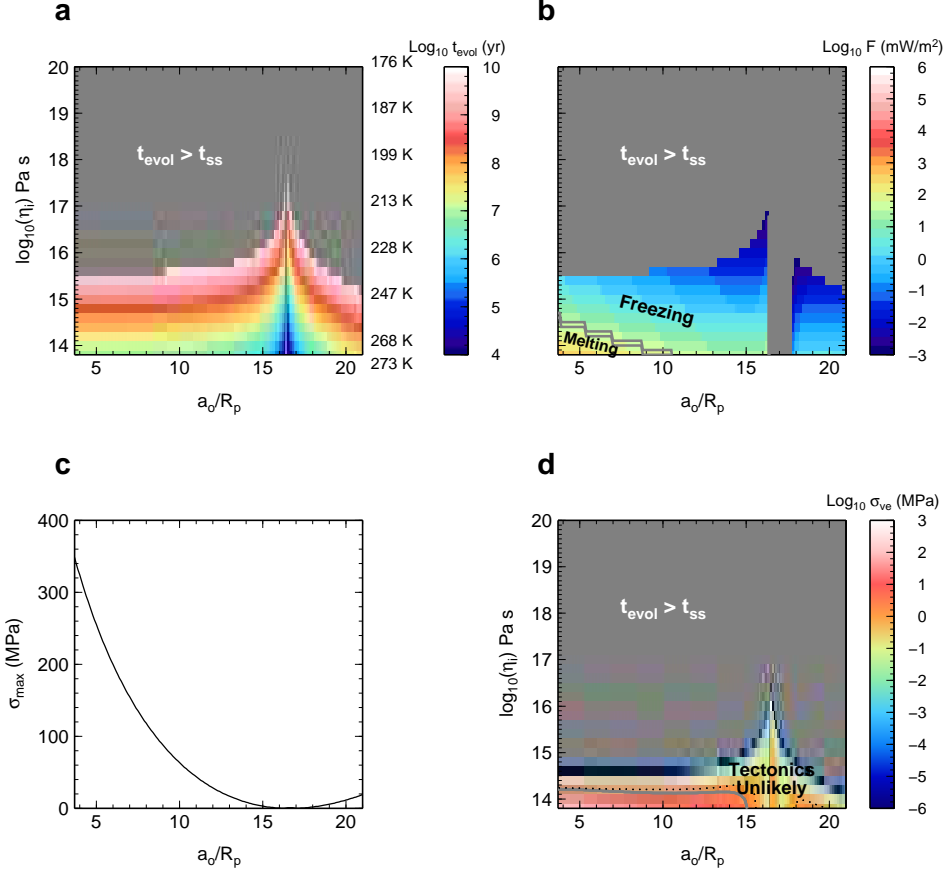


Figure 3: Orbital timescales and stresses, assuming Pluto does not have an ocean (see Figure 2b). (a) Time scale for Charon to evolve to the dual synchronous state ($a_o/R_p \sim 16.4$) depends strongly on the viscosity (η_i) of Pluto's ice shell (i.e., temperature, with approximate values shown on the right-hand axis, assuming a grain size $d = 0.1$ mm). To achieve t_{evol} (colors) less than the age of the solar system, Pluto's ice shell must be warmed to $T > 258$ K, assuming a minimum $d \sim 0.3$ mm. (b) Heat flux from tidal dissipation in Pluto during Charon's orbital evolution. If $F > F_{conv,max}$ (red/orange values), the ice shell will thin and become conductive. (c) Maximum tensile stress achievable due to despinning on Pluto, without regard to viscous relaxation. Larger stresses are associated with larger changes in Charon's orbital distance. (d) Maximum residual viscoelastic tensile stress remaining after time period of orbital evolution. The line between "Tectonics unlikely" and "Tectonics likely" is drawn along the 2.5 MPa contour. Dotted lines indicate a yield stress of 0.1 MPa, more appropriate for fractured ice (Beeman et al., 1988).

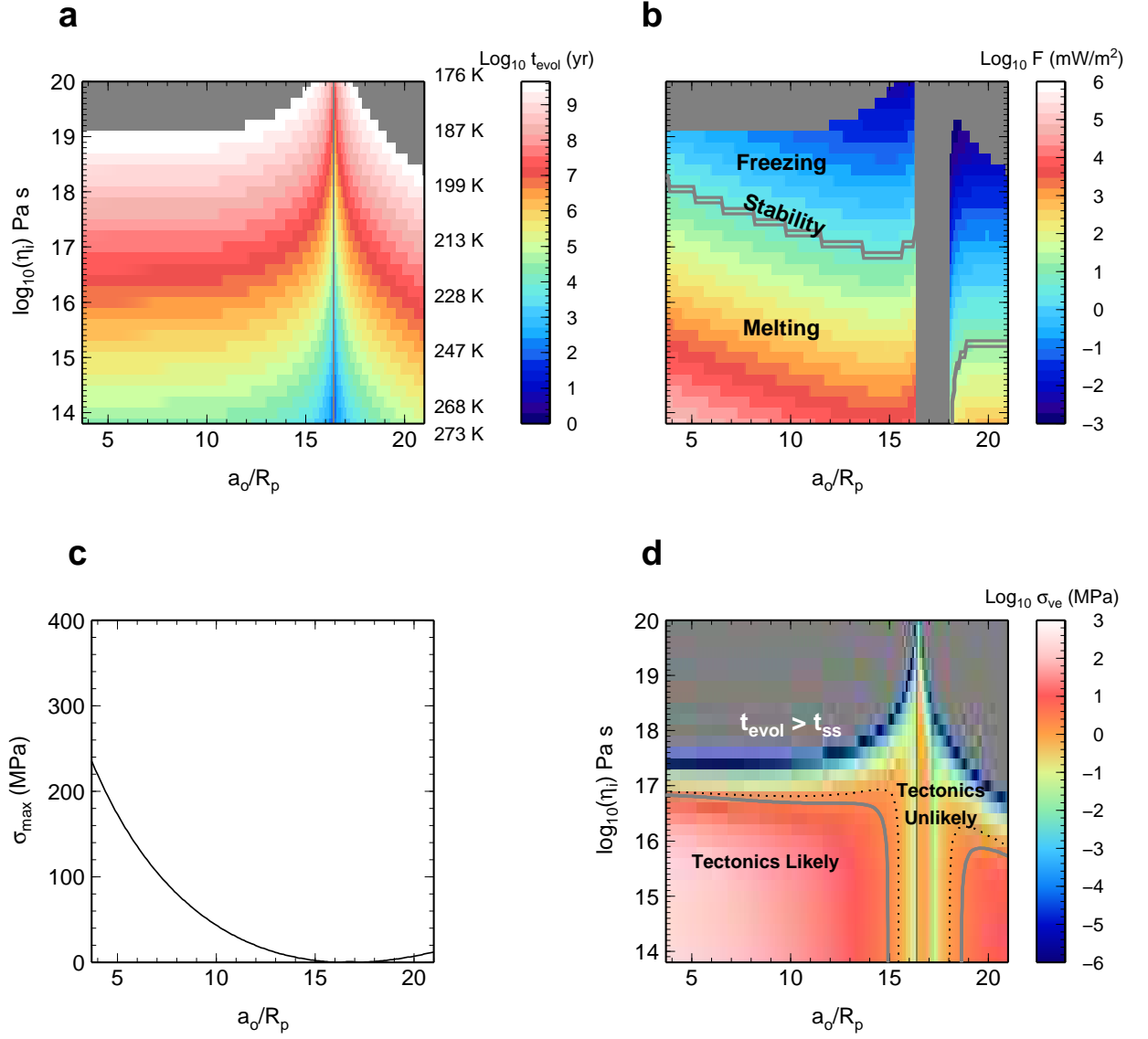


Figure 4: Similar to Figure 3, but for a uniform-density (undifferentiated) Pluto (interior structure shown in Figure 2c). (a) Time scale for orbital evolution. (b) Heat flux from tidal dissipation in Pluto. (c) Maximum despinning tensile stress achievable on Pluto. (d) Residual viscoelastic tensile stress after orbital evolution.

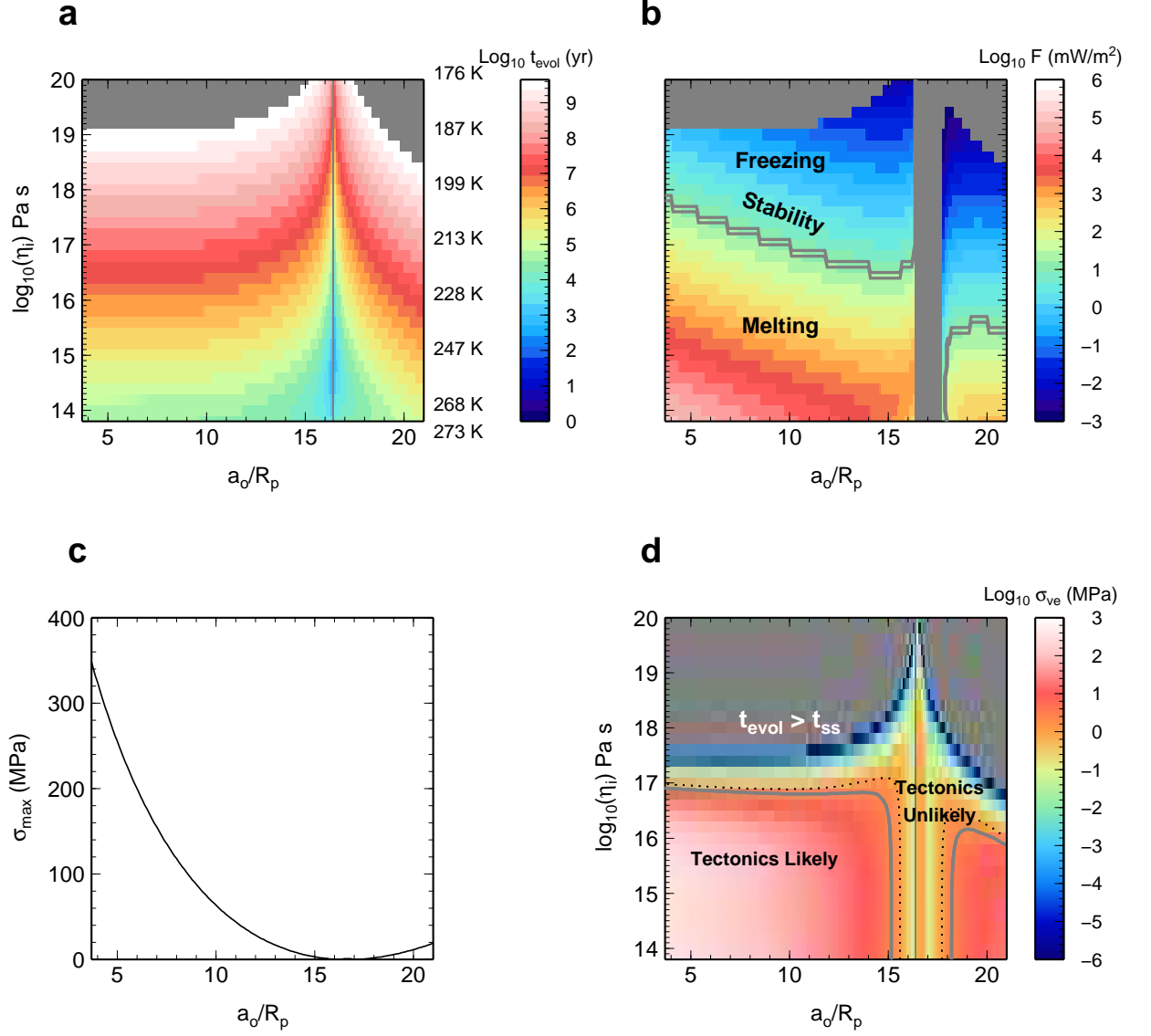


Figure 5: (a) Similar to Figure 3, but for a differentiated Pluto with an ocean (interior structure shown in Figure 2a). (a) Time scale for orbital evolution. (b) Heat flux from tidal dissipation in Pluto. (c) Maximum despinning tensile stress achievable on Pluto. (d) Residual viscoelastic tensile stress after orbital evolution.